JOURNAL OF AGRICULTURAL AND FOOD CHEMISTRY
ARTICLE

J. Agric. Food Chem. 2009, 57, 6871–6878 6871
DOI:10.1021/jf901461u

Fourier Transform Infrared Microspectroscopic Analysis of the Effects of Cereal Type and Variety within a Type of Grain on Structural Makeup in Relation to Rumen Degradation Kinetics

Amanda M. Walker, Peiqiang Yu, Colleen R. Christensen, David A. Christensen, and John J. McKinnon*

College of Agriculture and Bioresources, University of Saskatchewan, 51 Campus Drive, Saskatoon, Saskatchewan S7N 5A8, Canada

The objectives of this study were to use Fourier transform infrared microspectroscopy (FTIRM) to determine structural makeup (features) of cereal grain endosperm tissue and to reveal and identify differences in protein and carbohydrate structural makeup between different cereal types (corn vs barley) and between different varieties within a grain (barley CDC Bold, CDC Dolly, Harrington, and Valier). Another objective was to investigate how these structural features relate to rumen degradation kinetics. The items assessed included (1) structural differences in protein amide I to nonstructural carbohydrate (NSC, starch) intensity and ratio within cellular dimensions; (2) molecular structural differences in the secondary structure profile of protein, α-helix, β-sheet, and their ratio; (3) structural differences in NSC to amide I ratio profile. From the results, it was observed that (1) comparison between grain types [corn (cv. Pioneer 39P78) vs barley (cv. Harrington)] showed significant differences in structural makeup in terms of NSC, amide I to NSC ratio, and rumen degradation kinetics (degradation ratio, effective degradability of dry matter, protein and NSC) ($P < 0.05$); (2) comparison between varieties within a grain (barley varieties) also showed significant differences in structural makeup in terms of amide I, NSC, amide I to NSC ratio, α-helix and β-sheet protein structures, and rumen degradation kinetics (effective degradability of dry matter, protein, and NSC) ($P < 0.05$); (3) correlation analysis showed that the amide I to NSC ratio was strongly correlated with rumen degradation kinetics in terms of the degradation rate ($R = 0.91$, $P = 0.086$) and effective degradability of dry matter ($R = 0.93$, $P = 0.071$). The results suggest that with the FTIRM technique, the structural makeup differences between cereal types and between different varieties within a type of grain could be revealed. These structural makeup differences were related to the rate and extent of rumen degradation.

KEYWORDS: Infrared microspectroscopy; structural makeup; protein molecular structure; rumen degradation kinetics; cereal grains

INTRODUCTION

Cereal grains are the principal energy source in many animal diets. The endosperm is the largest tissue of the cereal grain kernel, accounting for nearly 80% of the total kernel weight (*1*), and because of its high nonstructural carbohydrate (NSC, starch) content, it also provides the majority of the energy to the animal. The nutritional value of the endosperm contributes significantly to the overall kernel digestibility. One of the most widely used methods of estimating rumen degradation kinetics of cereal grains is the in situ technique. However, this method tends to be labor-intensive and time-consuming. Furthermore, the "wet" chemical analysis of nutrient composition destroys the intrinsic structure of the grain tissue, eliminating the possibility of relating nutritional tissue content to in situ degradation kinetics.

Fourier transform infrared (IR) microspectroscopy (FTIRM) has the ability to identify chemical components within biological tissues based on the unique vibrational characteristics of molecules and bonds exposed to mid-IR radiation. IR spectroscopy with thermal IR sources has proven to be a valuable tool for resolving the molecular structural features (chemical makeup) in a wide range of biological materials, including plant and animal tissues (*2*−*10*). In the FTIRM technique, intact cross sections of tissues are used for analysis. This allows for the resolution of the structure and concentration of macromolecules present in cells and tissues. Consequently, it has the potential to analyze discrete and isolated areas of the grain kernel, such as the endosperm tissue, which cannot be accomplished with traditional "wet" chemistry methods of analysis because of damage during wet chemical analysis. Previous work (*3*, *4*, *6*) indicated that synchrotron-based FTIRM, which allows for IR analysis at

*Address correspondence to this author at the College of Agriculture and Bioresources, University of Saskatchewan 6D10 Agriculture Building, 51 Campus Dr., Saskatoon, SK S7N 5A8, Canada [telephone (306) 966-4137; fax (306) 966-4151; e-mail john.mckinnon@usask.ca].

Published on Web 07/10/2009

spatial resolutions approaching cellular dimensions, can be related to degradation kinetics in the rumen. The FTIRM technique can use either synchrotron or thermal-source IR light. One advantage of synchrotron-sourced FTIR microspectroscopy is increased brightness, which allows for better signal-to-noise at highly ultraspatial resolution (*4*, *5*, *7*−*9*). However, synchrotron-based FTIR studies can be expensive, and synchrotron facilities are limited. Thermal-sourced FTIRM, on the other hand, is more readily accessible and available.

There have been few publications on the application of FTIRM to the study of molecular structures or structural makeup in cereal grains in relation to nutrient variation and availability (*3*, *11*−*13*). Seed inherent structure, among other factors such as protein matrix, affects nutritive quality, fermentation, and degradation behavior in both humans and animals. The relative percentage of protein structures (amide I, α-helix, β-sheet, and their ratio) may influence protein functionality and value.

The objectives of this study were to use the FTIRM technique to determine structural features (makeup) of cereal grain endosperm tissues, to reveal and identify differences in protein and carbohydrate structural makeup between different cereal types (corn vs barley) and between different varieties within a grain (barley CDC Bold, CDC Dolly, Harrington, and Valier), and to investigate how these structural features relate to rumen degradation kinetics. The items assessed included (1) structural differences in protein amide I to nonstructural carbohydrate (NSC) intensity and ratio within cellular dimensions; (2) molecular structural differences in the secondary structure profile of protein, α-helix, β-sheet, and their ratio; and (3) structural differences in NSC to amide I ratio profile.

MATERIALS AND METHODS

Sample Preparation for FTIRM Spectral Analysis. Harrington (2-row malting barley), Valier (2-row midseason spring barley), CDC Bold (2-row hulled semidwarf feed barley), and CDC Dolly (2-row feed barley) were grown at the Crop Development Center, University of Saskatchewan (Saskatoon, SK, Canada), in 2006, and kept in dry storage at room temperature before analysis. Corn (cv. Pioneer 39P78) was obtained from the Prairie Feed Resource Centre (Saskatoon, SK, Canada). Five kernels of barley from each variety were selected on the basis of the diameter and weight parameters described in **Table 1**. Five corn kernels were visually assessed and selected from the weight range of 190−210 mg. Corn and barley seeds were imbibed in distilled water for 24 h at 4 °C and then frozen at −20 °C. Frozen seeds were cut into 6 μm sections using a cryostat (Leica CM3050S, Leica Microsystems, Wetzlar, Germany) and were dry-mounted onto Low-e IR microscope slides (Kevley Technologies, Chesterland, OH) for microspectroscopy in reflectance mode with thermal-sourced FTIRM.

FTIRM Spectral Data Collection. Thermal-sourced FTIRM was performed on the 01B1-1 mid-IR beamline at the Canadian Light Source (CLS, University of Saskatchewan, Saskatoon, Canada) using a Hyperion microscope with programmable mapping stage, a Bruker IFS 66v/S series IR spectrophotometer (Bruker Optics Inc., Billerica, MA), and the internal Globar IR light source. The aperture was set at 50 × 50 μm. Fifty discrete spot samples were collected from the endosperm region of five tissue sections of corn (cv. 39P78) and four barley varieties (cv. CDC Bold, CDC Dolly, Harrington, and Valier), for a total of 250 spectra from each grain variety. To ensure measurements were within the endosperm tissue, spot sample location was confined to the region extending 100−600 μm inside the aleurone layer in barley and within the vitreous endosperm region of corn. Spectral data were collected in the mid-infrared range of 4000−800 cm^{-1} at a wavelength resolution of 4 cm^{-1} and an aperture setting of 50 × 50 μm. Background and sample spectra consisted of 256 and 32 co-added scans, respectively.

Spectral Data Analysis. Automated stage control, spectrum data collection, and processing were performed using OPUS version 4.2 (Bruker Optics Inc.). Each sample spectrum was corrected by subtracting the corresponding background spectrum and displayed in absorbance mode. Automatic baseline correction was applied. Poor-quality spectra with high noise or high absorbance indicating detector saturation were removed from the data set prior to statistical analysis. Absorption peak area for amide I attributed to protein (1580−1710 cm^{-1}) and carbohydrate attributed to starch (1065−950 cm^{-1}) was calculated. NSC/amide I spectral peak area ratios were obtained by dividing the area under the NSC absorption peak (1065−950 cm^{-1}) by the area under the amide I absorption peak (1580−1710 cm^{-1}). **Figure 1** shows a typical IR spectrum and illustrates how peak area ratio was calculated in this experiment. The relative contribution of α-helix and β-sheet protein secondary structure to the amide I absorption band was determined by using the second-derivative spectrum to locate the α-helix (ca. 1655 cm^{-1}) and β-sheet (ca. 1630 cm^{-1}) component peaks (*13*). Hierarchical cluster analysis was performed on single-pixel spectra from corn and barley using Statistica software 6.0 (StatSoft Inc., Tulsa, OK).

Table 1. Seed Size and Weight Characteristics and Chemical Profiles of Corn and Barley Grain

	grain				
		barley			
item	corn	CDC Bold	CDC Dolly	Harrington	Valier
seed size (mm)		2.97−3.18	2.97−3.18	2.97−3.18	2.59−2.77
weight (mg)		54.0−54.9	56.0−56.9	53.0−53.9	47.6−48.5
chemical composition (g kg^{-1} of DM)					
dry matter	906	883	884	889	892
starch	665	633	587	578	566
CP	115	111	128	141	140
starch:protein	5.8	5.7	4.6	4.1	4.0

Sample Preparation for in Situ Kinetic Study. Prior to processing, barley samples were screened on 3.18, 2.97, 2.78, 2.59, and 2.38 mm screens using a Dockage Tester (Carter-Day Co., Minneapolis, MN) to remove seeds that would be differentially affected by processing. To minimize shattering, barley and corn samples were tempered for 24 h to a moisture content of 11−12% prior to processing using the tempering method for test milling wheat (26-10A) according to the American Association of Cereal Chemists (*14*). Samples were rolled using a Sven Roller Mill (Apollo Machine and Products Ltd., Saskatoon, SK) with 20 cm rollers adjusted to a gap size of 1.7 mm for Harrington, CDC Bold, and CDC Dolly and a 1.6 mm gap for Valier. Roller gap size was adjusted proportionately to the average plumpness of 100 kernels of each variety as measured with a caliper. Particle size of rolled barley was determined by dry sieving with an oscillating sieve shaker (RX-86 Sieve Shaker, W. S. Tyler, Mentor, OH) with sieves arranged in descending mesh size: 3.35, 2.36, 2.0, 1.4, and 1.0 mm and pan. The acceptable degree of processing was determined to contain < 30 g kg^{-1} fines characterized by the portion of sample collected in the pan (i.e., passing through 1 mm screen) (*15*).

Animals and Diets for in Situ Kinetics Study. Rumen degradation characteristics were determined using two ruminally cannulated yearling Angus heifers (400 kg). Animals were housed in individual 3 × 3 m pens with rubber floor mats and free access to water and were fed a ration consisting of 425 g kg^{-1} rolled corn, 425 g kg^{-1} rolled barley, and 150 g kg^{-1} barley silage on a DM basis. Feed was provided in two equal portions at 8:00 a.m. and 4:00 p.m. The daily ration included 55 g of mineral (CO-OP 3:1 Beef Cattle Mineral, Reg. 640314, Co-op Feeds, Ltd., Saskatoon, SK). Animals used in this experiment were cared for in accordance with the guidelines of the Canadian Council on Animal Care (*16*).

In Situ Rumen Incubation. Seven-gram samples of each test grain were weighed into 10 × 20 cm coded bags (Nitex 03-41/31 monofilament open mesh fabric, Screentec Corp., Mississauga, ON, Canada) with a pore size of 41 μm. Two separate trials were conducted: Trial 1 compared grain type effect (corn cv. Pioneer 39P78 vs barley cv. Harrington) , and trial 2 compared variety effect within a grain type (four barley varieties). Nylon bags were incubated in the rumen for 2, 4, 8, 12, 24, and 36 h in both trials 1 and 2. Two complete sets of the sample treatments were incubated in each animal for a total of four sets per trial. In situ incubation was

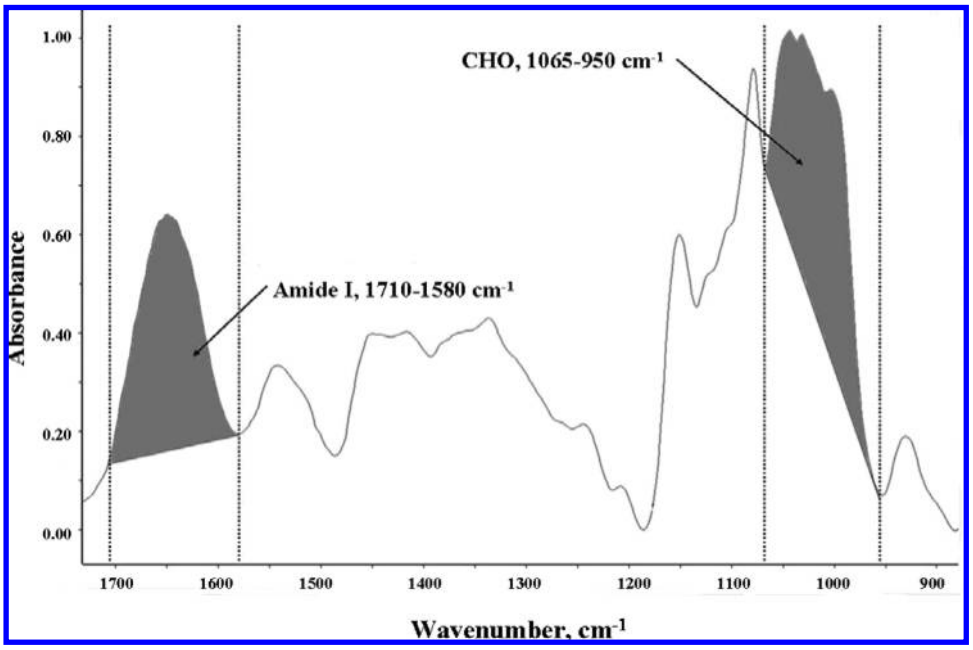

Figure 1. Typical internal IR-source FTIRM spectrum of cereal grain barley (cv. CDC Bold) in the 1700−900 cm^{-1} region illustrating the calculation of peak area under the absorption peak of amide I (1710−1580 cm^{-1}) and NSC (starch) (1065−950 cm^{-1}).

carried out according to the procedure described by McKinnon et al. (*17*). Dry sample residues were weighed for chemical analysis.

Chemical Analysis. Samples of the original and rumen residues were ground through a 0.5 mm screen using an ultracentrifugal mill (Retsch ZM 100, Haan, Germany) and analyzed for dry matter (DM) (AOAC method 954.02) and crude protein (CP) (AOAC method 984.13) according to the procedures of the AOAC (*18*). Total starch content was analyzed using the Megazyme Total Starch Assay Kit (Wicklow, Ireland) (AOAC method 996.11). Glucose concentration of each sample solution was measured with a spectrophotometer (Ultrospec III, Pharmacia LKB Biochrom, Ltd., Cambridge, U.K.). Absorbance of samples was read at 510 nm against a glucose standard processed under the same conditions.

Rumen Degradation Kinetics. In situ digestion kinetics were estimated according to the method of Yu et al. (*19*), using the proc NLIN procedure of the statistical package SAS 9.1 (*20*) with iterative least-squares regression (Gauss−Newton method). The percentages of DM, CP, and starch residue from each in situ incubation period were fitted to the first-order kinetics equation: $R(t) = U + D \times \exp^{(-K_d \times (t - t_0))}$ (*21*, *22*), where $R(t)$ = residue of the incubated material after t h of rumen incubation (g kg^{-1}); U = undegradable fraction (g kg^{-1}); D = potentially degradable fraction (g/kg); t_0 = lag time (h); and K_d = degradation rate (g kg^{-1} h^{-1}). Effective degradability of dry matter (EDDM), crude protein (EDCP), and starch (EDSt) were calculated as follows: EDDM, EDCP or EDSt (g/kg) = $S + D \times K_d/(K_p + K_d)$, where S = soluble (washable) fraction (g kg^{-1}), and K_p = estimated rate of outflow from the rumen (% h^{-1}). A K_p value of 6% h^{-1} was adopted to represent the rumen turnover rate (*19*).

Statistical Analysis. *Structural Makeup Study*. Statistical analyses were performed using the MIXED procedure of SAS (version 9.1.3) (*20*) using a completely randomized nested design. The model used for the analysis was $Y = \mu + \alpha + \beta(\alpha) + \varepsilon$, where Y is an observation of the dependent variable, μ is the population mean, α is the effect of grain variety, β is the effect of the seed section, and ε is the random error associated with the observation.

In Situ Rumen Kinetic Study. Statistical analyses were performed using the MIXED procedure of SAS (version 9.1.3) (*20*) using a completely randomized design. The model used for the analysis was $Y = \mu + \alpha + \varepsilon$, where Y is an observation of the dependent variable, μ is the population mean for the variable, α is the effect of grain type and grain variety, as a fixed effect, and ε is the random error associated with the observation. The effect of heifer was entered in the model as a random error term.

For all statistical analyses, significance was declared at $P < 0.05$. Differences between grain types and between varieties within the grain were evaluated using a multiple comparison test following Fisher's Protected LSD method (mean separation was done by using the PDIFF statement in SAS).

RESULTS AND DISCUSSION

Chemical Feature of Grain Kernel: Comparison between Grain Types and between Varieties within a Grain. The chemical composition of NSC-starch (non-structural carbyhydrate attributed to starch) and CP, and the ratio of whole-kernel NSC-starch to protein for corn and the four barley cultivars are shown in **Table 1**. Harrington and Valier barley had similar NSC-starch (578 and 566 g kg^{-1}, respectively) and CP (141 and 140 g kg^{-1}, respectively) contents, similar to the findings of Yu et al. (*19*). Numerically, CDC Bold had the highest NSC-starch content of the four barley varieties (633 g kg^{-1}), but the lowest CP (111 g kg^{-1}), resulting in the highest NSC-starch/protein ratio. CDC Dolly was intermediate for both starch and protein contents (587 and 128 g kg^{-1}, respectively). Corn had a higher starch content than all barley varieties and relatively low protein (115 g kg^{-1}), consequently giving it the highest NSC-starch/protein ratio.

The ratios presented in **Table 1** represent the relative amounts of NSC-starch and protein within the entire kernel rather than only a specific region due to the fact that wet chemical analysis procedures require homogenization of the sample tissue before analysis and destroy the inherent structural makeup during the chemical analysis.

Protein within the endosperm tissue of cereal grains is arranged in a matrix that surrounds and protects the starch granules, making them less available for digestion by rumen bacteria (*23*). Consequently, this is one factor responsible for differences in rumen starch degradation among different grain varieties. If more protein within the grain kernel equates to a more resistant protein matrix, then a higher protein content should indicate a larger degree of "protection", which would be related to a reduced rate and extent of starch degradation by rumen microbes. Therefore, a lower starch to protein ratio may correspond to a greater degree of protection for starch granules

within the protein matrix, resulting in a lower rate and extent of rumen degradation (*3*).

In Situ Rumen Degradation Kinetics: Comparison between Grain Types and between Varieties within a Grain. In situ rumen degradation kinetics of DM, CP, and starch between grain types (corn cv. P39P78 vs barley cv. Harrington) are reported in **Table 2**. Dry matter and NSC-starch in Harrington barley were degraded more quickly ($P < 0.05$) than in corn, and the extent of degradation (EDDM, EDCP, and EDST, which were obtained indirectly from a fit to the exponential equation) was higher ($P < 0.05$) for barley than for corn. There is limited in situ degradability data comparing rolled corn and barley in the literature; however, for in situ degradability experiments using ground samples, Herrera-Saldana et al. (*24*) and Boss and Bowman (*25*) found that ground barley was degraded more quickly and to a greater extent than corn. Solubility of DM and starch was not different between Harrington and corn, but the soluble fraction of CP was lower ($P < 0.05$) for rolled Harrington than for corn (39 vs 87 g kg^{-1}). The EDCP (343 vs 460 g kg^{-1}) and EDST (392 vs 614 g kg^{-1}) were lower for corn than for Harrington barley as a result of a slower K_d, leaving more material undegraded in the rumen and reducing the overall degradability. This is consistent with Orskov's observation that a greater proportion of barley starch is fermented in the rumen than that of corn (*26*).

In situ rumen degradation kinetics between varieties within barley grain (barley varieties CDC Bold, CDC Dolly, Harrington, and Valier) from trial 2 are presented in **Table 3**. Rates of DM degradation ranged from 13.7 to 16.6% h^{-1} and showed no statistical difference between the varieties ($P = 0.256$), similar to the observation of Ramsey et al. (*27*). Neither the present study nor that of Ramsey et al. (*27*) was able to detect any differences in K_d of DM and starch between different varieties of rolled barley. Similarly, Yu et al. (*3*) did not find differences in the K_d of DM, CP, or starch between rolled Harrington and Valier barley. Significant differences ($P < 0.05$) were detected in the *S* fraction of DM, CP, and starch between rolled barley varieties. Valier had lower ($P < 0.05$) solubility of DM, CP, and starch than both

Table 2. In Situ Rumen Degradation Kinetics of Grain Type: Comparison between Corn (Cv. P39P78) and Barley (Cv. Harrington) (Trial 1)[a]

	grain type			
item	corn	barley	SEM	*P* value
rumen degradation characteristics of DM				
degradation rate (K_d, % h^{-1})	8.9 a	12.1 b	1.33	0.005
lag time (t_0, h)	1.03	0.52	0.25	0.049
soluble fraction (*S*, g kg^{-1})	89	90	4.0	0.928
potentially degradable fraction (*D*, g kg^{-1})	505 b	660 a	20.1	0.003
undegradable fraction (*U*, g kg^{-1})	406 a	252 b	17.8	0.002
effective degradability of DM (EDDM, g kg^{-1})	382 b	527 a	8.1	<0.001
rumen degradation characteristics of crude protein (CP)				
degradation rate (K_d, % h^{-1})	6.2	8.7	0.97	0.114
lag time (t_0, h)	0.87	0.67	0.288	0.357
soluble fraction (*S*, g kg^{-1})	87 a	39 b	13.4	0.044
potentially degradable fraction (*D*, g kg^{-1})	510 b	722 a	22.8	0.001
undegradable fraction (*U*, g kg^{-1})	402 a	239 b	21.6	0.001
effective degradability of CP (EDCP, g kg^{-1})	343 b	460 a	5.9	<0.001
rumen degradation characteristics of starch (St)				
degradation rate (K_d, % h^{-1})	10.7 b	16.2 a	1.78	0.049
lag time (t_0, h)	1.63	0.64	0.45	0.212
soluble fraction (*S*, g kg^{-1})	557	73	11.9	0.196
potentially degradable fraction (*D*, g kg^{-1})	527 b	753 a	22.2	<0.001
undegradable fraction (*U*, g kg^{-1})	417 a	174 b	19.3	<0.001
effective degradability of ST (EDSt, g kg^{-1})	392 b	614 a	8.9	<0.001

[a] Within a row, means with different letters are significantly different ($P < 0.05$).

Table 4. Protein Amide I and Nonstructural Carbohydrate (NSC, Starch) Mid-Infrared Absorption Using FTIR Microspectroscopy: Comparison between Barley (Cv. Harrington) and Corn (Cv. P39P78)[a]

	infrared absorption intensity units[b]		
grain type	amide I (±SD)	NSC (±SD)	NSC/amide I (±SD)
barley	24.4 (±7.6)	22.0 (±6.6) b	0.99 (±0.43) b
corn	24.0 (±7.5)	43.7 (±10.6) a	1.96 (±0.73) a
SEM	0.53	0.60	0.036
P value	0.600	<0.001	<0.001

[a] Within a column, means with different letters are significantly different ($P < 0.05$). [b] Absorption peak area for amide I attributed to protein (1580−1710 cm^{-1}) and that for carbohydrate attributed to starch (1065−950 cm^{-1}).

Table 3. In Situ Rumen Degradation Kinetics of Barley: Comparison among CDC Bold, CDC Dolly, Harrington, and Valier Barley (Trial 2)[a]

	barley variety					
item	Bold	Dolly	Harrington	Valier	SEM	*P* value
rumen degradation characteristics of dry matter (DM)						
degradation rate (K_d, % h^{-1})	16.6	15.8	14.9	13.7	0.98	0.256
lag time (t_0, h)	0.00	0.00	0.00	0.06	0.020	0.138
soluble fraction (*S*, g kg^{-1})	105 a	93 a	94 a	67 b	7.5	0.005
potentially degradable fraction (*D*, g kg^{-1})	705	718	702	697	13.7	0.677
effective degradability of DM (EDDM, g kg^{-1})	622 a	610 ab	593 b	550 c	15.0	0.001
rumen degradation characteristics of crude protein (CP)						
degradation rate (K_d, % h^{-1})	12.2	11.8	10.1	10.2	0.80	0.184
lag time (t_0, h)	0.00	0.00	0.00	0.06	0.026	0.329
soluble fraction (*S*, g kg^{-1})	70 a	47 ab	28 bc	5 c	8.7	0.015
potentially degradable fraction (*D*, g kg^{-1})	778	796	787	781	23.9	0.903
effective degradability of CP (EDCP, g kg^{-1})	592 a	572 a	520 b	485 c	13.3	<0.001
rumen degradation characteristics of starch						
degradation rate (K_d, % h^{-1})	17.0	16.6	16.7	14.8	0.86	0.299
lag time (t_0, h)	0.00 b	0.00 b	0.00 b	0.10 a	0.018	0.010
soluble fraction (*S*, g kg^{-1})	114 a	84 ab	68 bc	40 c	12.5	0.014
potentially degradable fraction (*D*, g kg^{-1})	819	852	835	853	16.4	0.392
effective degradability of ST (EDST, g kg^{-1})	719 a	708 ab	680 b	644 c	17.4	0.002

[a] Within a row, means with different letters are significantly different ($P < 0.05$).

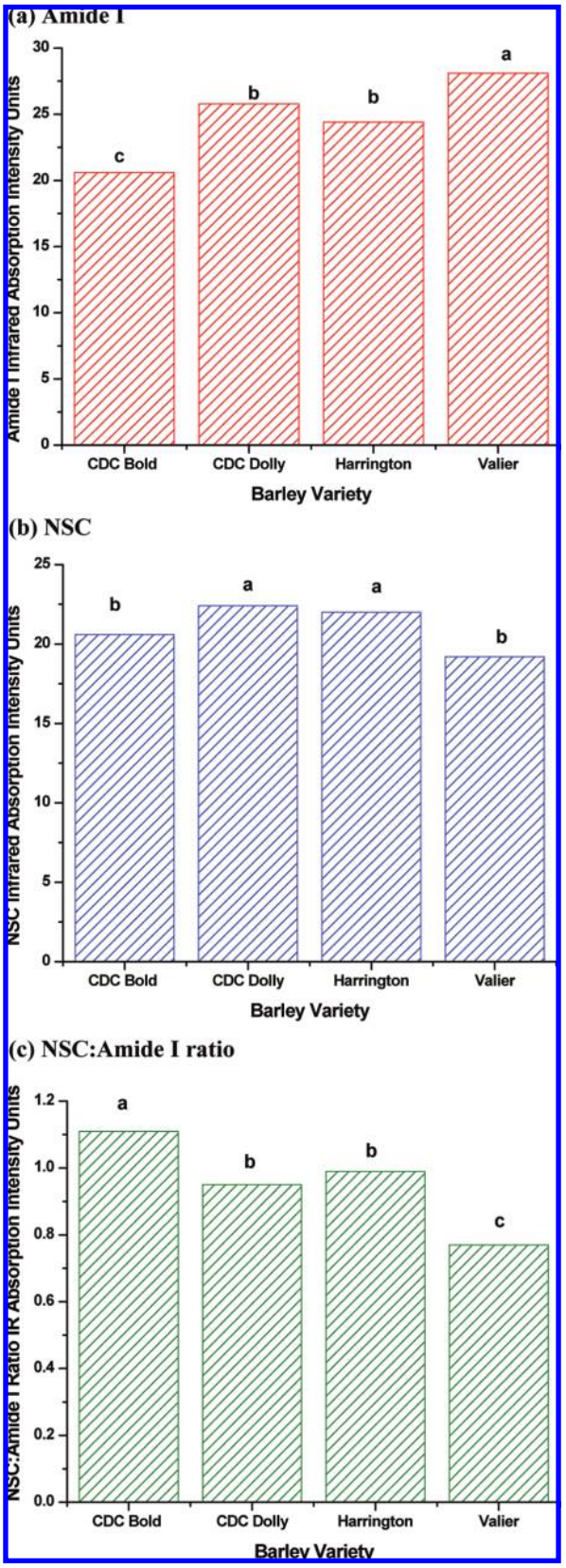

Figure 2. Protein amide I (**a**), nonstructural carbohydrate (NSC, starch) (**b**), and NSC/amide I ratio (**c**) mid-infrared absorption of barley using FTIR microspectroscopy: comparison among CDC Bold, CDC Dolly, Harrington, and Valier barley. Absorption peak area for amide I attributed to protein (1580−1710 cm^{-1}) and that for carbohydrate attributed to NSC starch (1065−950 cm^{-1}).

CDC Bold and CDC Dolly and was similar to Harrington for CP and starch solubility (**Table 3**). Valier had lower EDDM, EDCP, and EDSt than CDC Bold and CDC Dolly (**Table 3**), indicating less extensive rumen fermentation despite the fact that the actual rate of degradation was similar. Reduction in the extent of starch degradation exhibited by Valier barley may be caused in part by lower CP solubility. Reduced CP solubility may indicate that the protein matrix has not been disrupted to the same extent and is therefore more effective in reducing the extent of starch degradation.

Table 5. Pearson Correlation Coefficients between NSC/Amide I Ratio Determined Using FTIRM and in Situ Rumen Degradation Characteristics of Dry Matter for Four Varieties of Barley: CDC Bold, CDC Dolly, Harrington, and Valier

	NSC/amide I ratio	
parameter	*R*	*P* value
degradation rate (K_d)	0.914	0.086
soluble fraction (*S*)	0.985	0.015
potentially degradable fraction (*D*)	0.346	0.654
undegradable fraction (*U*)	−0.876	0.124
effective degradability of DM (EDDM)	0.929	0.071

Despite the lack of significant differences in K_d, the ranking of barley varieties in the order of decreasing K_d corresponded to the order of decreasing starch/protein ratio in the kernel as estimated by chemical analysis (**Table 1**) (CDC Bold > CDC Dolly > Harrington > Valier). This suggests that a lower starch/protein ratio may be an indication of slower rumen degradation in barley.

Structural Feature (Makeup): Comparison between Grain Types and between Varieties within a Grain. In this analysis, the endosperm tissue was chosen as the site of analysis for two reasons. First, the endosperm comprises approximately 80% of the total kernel weight, so its structure (chemical makeup) contributes significantly to the overall kernel properties; second, isolating the endosperm region for FTIR analysis results in a more homogeneous tissue for spectral analysis.

Each biological component in seed tissue has unique molecular and chemical structural features; therefore, each has its own unique IR spectrum. The protein IR spectrum has two primary features, the protein amide I (ca. 1600−1700 cm^{-1}) and amide II (ca. 1500−1560 cm^{-1}) bands. These arise from specific stretching and bending vibrations of the protein backbone. The amide I band arises predominantly from the C═O stretching vibration (80%) of the amide C═O group plus C—N stretching vibration (*2*, *7*). Least-squares means of spectral peak area attributed to amide I (1580−1710 cm^{-1}) and NSC (1065−950 cm^{-1}) and ratios of NSC/amide I are shown in **Table 4**. The ratio of peak area for NSC/amide I was used for comparison of spectral data as differences in the IR absorbance that occur as a result of variation in tissue thickness can be accounted for by using peak height or area ratios (*28*).

The ratio of NSC/amide I peak area absorption within the endosperm was higher ($P < 0.05$) for corn than for Harrington barley (**Table 4**), consistent with the higher NSC/protein ratio of the whole corn kernel estimated by chemical analysis (**Table 1**). Despite exhibiting a slower K_d, corn had a higher NSC-starch/protein ratio in both the chemical analysis and FTIR analysis. Corn starch was more slowly digested even though there is relatively less protein present in the entire corn kernel as well as in the endosperm tissue. The higher rumen undegradable starch fraction of corn has been attributed to the interaction of starch and protein in the endosperm. The protein matrix surrounding starch granules in the endosperm serves to hinder bacterial attachment and digestion of starch granules by rumen microorganisms. It has been suggested that this protective action of protein has a greater effect on reducing the bacterial digestion

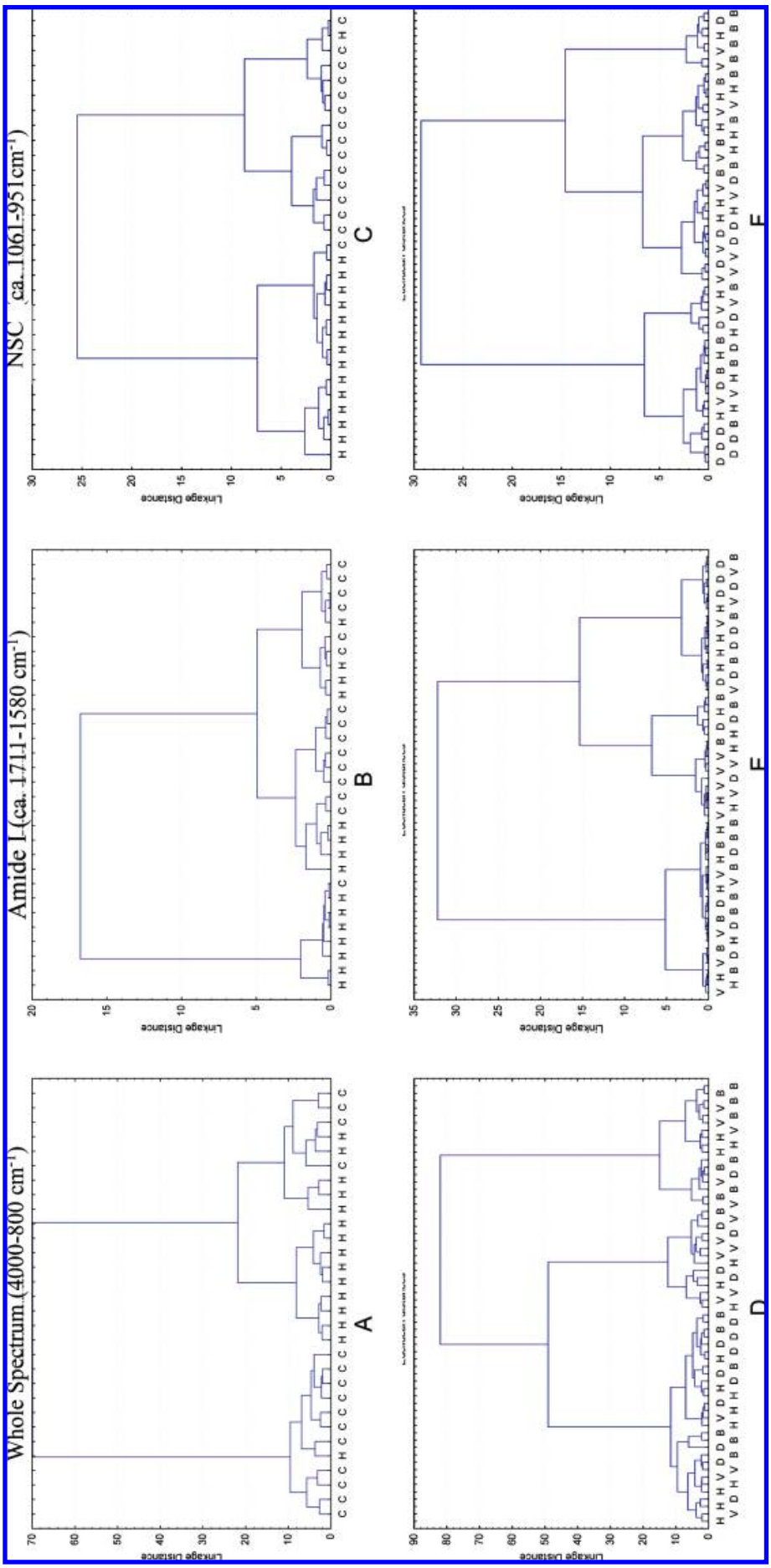

Figure 3. Multivariate spectral analysis of endosperm tissue of corn and barley: cluster analysis of whole spectrum (ca. 4000−800 cm^{-1}) for corn and Harrington barley (**A**) and Bold, Dolly, Harrington, and Valier barley (**B**); cluster analysis of amide I spectral region (ca. 1711−1580 cm^{-1}) for corn and Harrington barley (**B**) and four barley varieties (**E**); cluster analysis of CHO spectral region (ca. 1061−951 cm^{-1}) for corn and Harrington barley (**C**) and four barley varieties (**F**). C = corn; H = Harrington, B = Bold, D = Dolly, V = Valier.

of starch in corn than in barley (*23*). However, whereas the results of this work show that corn starch is more slowly degraded, the starch/protein ratio of the endosperm is greater than that of the more rapidly degraded Harrington barley. It is possible that the protective effect of protein is not due to the relative amount of protein in the endosperm, but due to differences in the protein type and structure. Corn and barley contain different amounts and types of the four major groups of cereal proteins: albumins, globulins, prolamins, and glutelins (*29*, *30*). Variation in the amino acid content and structure of these different proteins may influence how polypeptides react to degradation in the rumen environment, contributing to the observed differences in starch degradability in corn and barley seen in this study.

Comparison among CDC Bold, CDC Dolly, Harrington, and Valier barley in amide I, NSC, and NSC/amide I ratio of mid-infrared absorption of barley is presented in **Figure 2**. There was a wide variation in the spectral absorption intensity of peaks attributed to amide I and NSC. Harrington had a higher mean ($P < 0.05$) absorbance intensity than Valier for starch (22.0 vs 19.2, respectively) and a lower spectral absorbance intensity for amide I (24.4 vs 28.1, respectively). Similarly, Yu et al. observed that Harrington tended to have higher starch and lower protein absorbance intensity than Valier (*3*). CDC Bold had the largest NSC/amide I ratio (1.109), followed by CDC Dolly and Harrington (0.947 and 0.993, respectively) and Valier (0.767). This order of ranking is similar to that of the starch/protein ratio determined by chemical analysis (**Table 1**) and is also consistent with the results of the in situ rumen degradation kinetics, where CDC Bold had the greatest extent of rumen degradation ($P < 0.05$), followed by CDC Dolly, Harrington, and Valier (**Table 3**). Therefore, a lower NSC/amide I ratio measured by thermal-source FTIRM data seems to be associated with a lesser extent of rumen degradation among barley varieties.

Correlation Analysis between Structure Spectral Features and in Situ Rumen Degradation Kinetics. Table 5 shows the Pearson correlation coefficients between the ratio of NSC/amide I estimated with FTIRM and in situ rumen degradation kinetics of DM (K_d, S, D, U, EDDM) for the four barley varieties. The positive correlations between NSC/amide I ratio and both rate (K_d) and extent (EDDM) of rumen degradation approach significance ($P = 0.09$ and 0.07, respectively). There is a significant positive correlation between NSC/amide I and S fractions of DM. To more accurately test this relationship, IR analysis of additional barley and corn varieties would be beneficial, along with an increase in the number of corn samples to observe variation among different varieties of corn as seen with the barley varieties in this experiment.

Hierarchical Cluster Analysis To Discriminate and Classify Structural Makeup. Multivariate hierarchical cluster analysis was performed to compare structure differences between grain types (corn grain vs barley grain) and between varieties of barley (**Figure 3**) and to determine if the spectra could be statistically separated into distinct clusters based on qualitative spectral differences (*31*). Three spectral ranges were compared: (1) whole spectrum (ca. 4000−800 cm^{-1}), (2) the amide I spectral region (ca. 1710−1580 cm^{-1}), and (3) the NSC spectral region (ca. 1065−950 cm^{-1}). Whole spectrum analysis of corn versus Harrington showed nearly complete separation with the exception of one case of Harrington in the corn cluster and four cases of corn in the Harrington cluster. The analysis of the amide I region showed no separation of corn and Harrington; however, the clusters did show clear separation (with the exception of one case) between the NSC spectral regions. This indicated differences in the carbohydrate profile between corn and Harrington barley, similar to the differences observed in the FTIR starch absorbance data and NSC/amide I ratio (**Table 4**). When the spectral differences between the four barley varieties were examined, cluster analysis revealed no separation between whole spectrum, amide I, or NSC regions of different varieties.

Table 6. Effect of Barley Variety on Molecular Protein Structure Profile Determined Using FTIR Absorbance of α-Helix and β-Sheet Peaks within the Amide I Absorption Band[a]

	molecular protein structure (absorbance units)		
variety	α-helix (peak height)	β-sheet (peak height)	ratio of α-helix to β-sheet
Bold	0.8768 a	0.8809 a	1.0498
Dolly	0.6721 b	0.6589 b	1.0390
Harrington	0.6993 b	0.6269 b	1.0473
Valier	0.7267 b	0.7305 b	1.0469
SEM	0.0447	0.0499	0.0117
P value	0.0092	0.0038	0.929

[a] Within a column, means with different letters are significantly different ($P < 0.05$).

Protein Molecular Structure Difference: Comparison between Varieties within a Grain. The vibrational frequency of the amide I band is particularly sensitive to protein secondary structure; this can be used to determine secondary structure of proteins. For the α-helix, the amide I typically is in the range of ca. 1648−1658 cm^{-1}. For β-sheet, the peak falls within the range of 1620−1640 cm^{-1}. The amide II (predominantly an N−H bending vibration (60%) coupled to C−N stretching (40%)) also can be used to assess protein conformation and protein molecular chemical makeup. However, it arises from complex vibrations involving multiple functional groups, and it is less useful for protein structure prediction than the protein amide I band (*2*, *31*−*33*).

The amide I spectral absorption region of the original spectra was further analyzed to determine the proportions of α-helix and β-sheet secondary structures. Second derivatives were used to determine the presence and location of component peaks at ca. 1655 cm^{-1} for α-helix and ca. 1630 cm^{-1} for β-sheet (*32*, *33*). The spectra from corn did not display any peaks representing β-sheet absorption; all four barley varieties contained both α-helix and β-sheet peaks. No differences in the ratio of α-helix to β-sheet between the four barley varieties were observed (**Table 6**), but CDC Bold had the highest α-helix peak height ($P < 0.05$) among the barley varieties. Because CDC Bold also had the highest effective degradability of crude protein (**Table 3**), there could be some association between the content of α-helix structures and protein degradability.

In conclusion, comparison between grain types (corn cv. Pioneer 39P78 vs barley cv. Harrington) shows significant differences ($P < 0.05$) in structural features (makeup) in terms of NSC, amide I to NSC ratio, and rumen degradation kinetics (degradation ratio, effective degradability of dry matter, protein, and NSC). Comparison between the varieties within the barley grain revealed that there were also significant differences in structural features in terms of amide I, NSC, NSC/amide I ratio, α-helix protein structure, β-sheet protein structure, and rumen degradation kinetics (effective degradability of dry matter, protein, and NSC). Correlation analysis showed that the NSC/amide I ratio was correlated with rumen degradation kinetics in terms of the degradation rate ($R = 0.91$, $P = 0.086$) and effective degradability of dry matter ($R = 0.93$, $P = 0.071$). The results suggest that with the FTIRM technique, the structure differences between cereal types and between different varieties within a type of grain could be detected. These structure differences were related to the rate and extent of rumen degradation.

ACKNOWLEDGMENT

We thank Canadian Light Source (CLS, University of Saskatchewan, Saskatoon, Canada) for provision of experimental beamtime and acknowledge Dr. Tim May, who provided expertise on the 01B1-1 beamline.

LITERATURE CITED

(1) McAllister, T. A.; Cheng, K.-J. Microbial strategies in the ruminal digestion of cereal grains. *Anim. Feed Sci. Technol.* **1996**, *62*, 29–36.

(2) Jackson, M.; Mantsch, H. H. Medical science applications of IR. In *Encyclopedia of Spectroscopy and Spectrometry*; Tranter, G., Holmes, J., Lindon, J., Eds.; Academic Press: London, U.K., 1999; pp 1271−1281.

(3) Yu, P.; Christensen, D. A.; Christensen, C. R.; Drew, M. D.; Rossnagel, B. G.; McKinnon, J. J. Use of synchrotron FTIR microspectroscopy to identify chemical differences in barley endosperm tissue in relation to rumen degradation characteristics. *Can. J. Anim. Sci.* **2004**, *84*, 523–527.

(4) Yu, P.; McKinnon, J. J.; Christensen, C. R.; Christensen, D. A.; Marinkovic, N. S.; Miller, L. M. Chemical imaging of microstructures of plant tissues within cellular dimension using synchrotron infrared microspectroscopy. *J. Agric. Food Chem.* **2003**, *51*, 6062–6067.

(5) Miller, L. M.; Carr, G. L.; Jackson, M.; Dumas, P.; Williams, G. P. The impact of infrared synchrotron radiation in biology: past, present and future. *Synchrontron Radiat. News* **2000**, *13*, 31–38.

(6) Yu, P.; Jonkera, A.; Gruber, M. Molecular basis of protein structure in proanthocyanidin and anthocyanin-enhanced Lc-transgenic alfalfa in relation to nutritive value using synchrotron-radiation FTIR microspectroscopy: a novel approach. *Spectrochim. Acta Part A: Mol. Biomol. Spectrosc.* **2009**, *73*, 846–853.

(7) Marinkovic, N. S.; Chance, M. R. Synchrotron infrared microspectroscopy. In *Encyclopedia of Molecular Cell Biology and Molecular Medicine*, 2nd ed.; Meyers, R., Ed.; Wiley: New York, 2005; Vol. *13*, pp 671−708.

(8) Miller, L. M.; Dumas, P. Chemical imaging of biological tissue with synchrotron infrared light. *Biochim. Biophys. Acta* **2006**, *1758*, 846–857.

(9) Wetzel, D. L.; Srivarin, P.; Finney, J. R. Revealing protein infrared spectral detail in a heterogeneous matrix dominated by starch. *Vib. Spectrosc.* **2003**, *31*, 109–114.

(10) Marcott, C.; Reeder, R. C.; Sweat, J. A.; Panzer, D. D.; Wetzel, D. L. FT-IR spectroscopic imaging microscopy of wheat kernels using a mercury−cadmium−telluride focal-plane array detector. *Vib. Spectrosc.* **1999**, *19*, 123–129.

(11) Doiron, K. J.; Yu, P.; McKinnon, J. J.; Christensen, D. A. Heat-induced protein structures and protein subfractions in relation to protein degradation kinetics and intestinal availability in dairy cattle. *J. Dairy Sci.* **2009**, in press.

(12) Yu, P.; Block, H.; Niu, Z.; Doiron, K. Rapid characterization of molecular chemistry and nutrient make-up and microlocalization of internal seed tissue. *J. Synchrotron Radiat.* **2007**, *14*, 382–390.

(13) Yu, P. Molecular chemical structure of barley protein revealed by ultra-spatially resolved synchrotron light sourced FTIR microspectroscopy: comparison of barley varieties. *Biopolymers* **2006**, *85*, 308–317.

(14) American Association of Cereal Chemists. *Approved Methods of the American Association of Cereal Chemists*, 9th ed.; American Association of Cereal Chemists: St. Paul, MN, 1995.

(15) Mathison, G. W. *Processing Feed Grains*, Section 1, Factsheet 2, Alberta Feedlot Management Guide.

(16) Canadian Council on Animal Care. *Guide to the Care and Use of Experimental Animals*, 2nd ed.; Canadian Council on Animal Care: Ottawa, Canada, 1993; Vol. *1*.

(17) McKinnon, J. J.; Olubobokun, J. A.; Christensen, D. A.; Cohen, R. D. H. The influence of heat and chemical treatment on ruminal disappearance of canola meal. *Can. J. Anim. Sci.* **1991**, *71*, 773–780.

(18) Association of Analytical Chemists. *Official Methods of Analysis*, 15th ed.; AOAC: Arlington, VA, 1990.

(19) Yu, P.; Meier, J. A.; Christensen, D. A.; Rossnagel, B. G.; McKinnon, J. J. Using the NRC-2001 model and the DVE/OEB system to evaluate nutritive values of Harrington (malting-type) and Valier (feed-type) barley for ruminants. *Anim. Feed Sci. Technol.* **2003**, *107*, 45–60.

(20) Statistical Analysis System Institute. *SAS/STAT User's Guide*; SAS Institute: Cary, NC, 2003; version 9.1.3.

(21) Mertens, D. R.; Loften, J. R. The effect of starch on forage fiber digestion kinetics in vitro. *J. Dairy Sci.* **1980**, *63*, 1437–1446.

(22) Tamminga, S.; Van Straalen, W. M.; Subnel, A. P. J.; Meijer, R. G. M.; Steg, A.; Wever, C. J. G.; Blok, M. C. The Dutch protein evaluation system: the DVE/OEB-system. *Livest. Prod. Sci.* **1994**, *40*, 139–155.

(23) McAllister, T. A.; Phillippe, R. C.; Rode, L. M.; Cheng, K.-J. Effect of the protein matrix on the digestion of cereal grains by ruminal microorganisms. *J. Anim Sci.* **1993**, *71*, 205–212.

(24) Herrera-Saldana, R. E.; Huber, J. T.; Poore, M. H. Dry matter, crude protein, and starch degradability of five cereal grains. *J. Dairy Sci.* **1990**, *73*, 2386–2393.

(25) Boss, D. L.; Bowman, J. G. P. Barley varieties for finishing steers: II. Ruminal characteristics and rate, site, and extent of digestion. *J. Anim. Sci.* **1981**, *74*, 1973–1981.

(26) Orskov, E. R. Starch digestion and utilization in ruminants. *J. Anim. Sci.* **1986**, *63*, 1624–1633.

(27) Ramsey, P. B.; Mathison, G. W.; Goonewardene, L. A. Relationships between ruminal dry matter and starch disappearance and apparent digestibility of barley grain. *Anim. Feed Sci. Technol.* **2001**, *94*, 155–170.

(28) Miller, L. M. *Infrared Microspectroscopy and Imaging*; http://nslsweb.nsls.bnl.gov/nsls/pubs/nslspubs/imaging0502/irxrayworkshop introduction.ht (accessed Oct 2009).

(29) Lookhart, G. L.; Bean, S. Cereal proteins: Composition of their major fractions and methods for identification. In *Handbook of Cereal Science and Technology*; Kulp, K., Ponte, J. G., Jr., Eds.; Dekker: New York, 2000; pp 363−383.

(30) Shewry, P. R. Cereal grain proteins. In *Cereal Grain Quality*; Henry, R. J., Kettlewell, P. S., Eds.; Chapman and Hall: Cambridge, U.K., 1996; pp 227−244.

(31) Yu, P. Synchrotron IR microspectroscopy for protein structure analysis: potential and questions. *Spectroscopy* **2006**, *20*, 229–251.

(32) Marinkovic, N. S.; Huang, R.; Bromberg, P.; Sullivan, M.; Toomey, J.; Miller, L. M.; Sperber, E.; Moshe, S.; Jones, K. W.; Chouparowa, E.; Lappe, S.; Franzen, S.; Chance, M. R. Center for Synchrotron Biosciences' U2B beamline: an international resource for biological infrared spectroscopy. *J. Synchrotron Radiat.* **2002**, *9*, 187–189.

(33) Jackson, M.; Mantsch, H. H. The use and misuse of FTIR spectroscopy in the determination of protein structure. *Crit. Rev. Biochem. Mol. Biol.* **1995**, *30*, 95–120.

Received May 1, 2009. Revised manuscript received June 24, 2009. Accepted June 25, 2009. This study was supported by NSERC (National Sciences and Engineering Research Council of Canada) and Saskatchewan ADF.